H_2 Elimination from Hydrated Aluminum Clusters: Acid−Base Reaction Mediated by Intracluster Proton Transfer

Björn M. Reinhard* and Gereon Niedner-Schatteburg*

Fachbereich Chemie, Universität Kaiserslautern, 67663 Kaiserslautern, Germany

Received: March 27, 2002

The reactivity of different $[Al,20H_2O]^+$ clusters was investigated using gradient-corrected DFT. In clusters with the stoichiometry $[AlH(OH)(H_2O)_{19}]^+$, which contain a four-fold-coordinated Al^{III}, H_2 formation was found to occur according to the following mechanism: First a proton is released within the cluster by hydrolysis of a first shell H_2O. By successive proton-transfer reactions in the hydrogen-bonded network of the cluster, the proton migrates to the hydridic H at the Al^{III} cation. Finally, hydride ion and proton recombine to H_2 in an acid−base reaction. The activation barrier for this process was determined to be 45 kJ mol^{-1}. No H_2 formation was found in hydrated Al^I clusters, $[Al^I(H_2O)_{20}]^+$.

Introduction

Al^{III} hydrates in bulk phase through hexacoordination and yields the aqua ion $[Al^{III}(H_2O)_6]^{3+}$. This ion is acidic (pK_a = 4.56)

$$[Al^{III}(H_2O)_6]^{3+} \rightleftarrows [Al^{III}(H_2O)_5OH]^{2+} + H^+_{aq}$$

and the dication has been detected in dilute solution.[1] Over a wide pH range and in "physiological" chloride solutions, the monomeric Al^{III} species seem to be $[Al(OH)]^{2+}$, $Al(OH)_3$, and most evidently $[Al(OH)_4]^-$.[2] In particular, no indication of coordination with more than four hydroxide ligands was found. Similarly, the aluminum hydride anion $[AlH_4]^-$ shows tetrahedral coordination with an average Al−H distance of 1.55 Å in the crystalline $LiAlH_4$ solid. It explosively hydrolyzes by water.

Ionic water clusters are expected to resemble closely the solvation of ions in aqueous bulk-phase solution and act as model systems for solvation processes. They offer an approach to ionic species, which are not stable in the bulk phase, where they only exist as reactive intermediates for a very limited period of time. The study of these entities in the gas phase offers knowledge of fundamental chemical processes such as oxidation and solvation. Example par excellence for these species is the hydrated magnesium monocation, $[Mg(H_2O)_n]^+$. According to textbook inorganic chemistry, a hydrated Mg^I monocation does not exist. While this statement almost certainly holds in the bulk phase, it needed verification in the case of finite-size gas-phase clusters. Only recently calculations revealed that the oxidation state of the hydrated magnesium ion gradually increases as a function of cluster size, n.[3] While for $n < 6$ the odd electron is still located at the magnesium ion Mg^I within a sp-hybrid-like orbital, in larger clusters it is transferred into the outer solvation shell. This results in the coexistence of metal dication Mg^{II} and a hydrated electron within these clusters. In case of $[Mg(H_2O)_n]^+$, two different decay pathways were observed: reactive decay by H atom elimination and nonreactive decay by evaporation of a H_2O monomer.[4,5] The branching ratio was found to depend critically on the cluster size. The reactive decay pathway is confined to the cluster size regime $[Mg(H_2O)_n]^+$, n = 7−17. All other cluster sizes decay by evaporation.

In hydrated aluminum clusters, $[Al,20H_2O]^+$, two competing decay pathways occur as well. In their blackbody radiation-induced decay (BIRD) studies, Bondybey and co-workers observed a reactive decay by elimination of H_2 molecules, as well as decay solely by evaporation of H_2O.[6,7] In this case, the reactive decay pathway is confined to a size region of n = 11−24 and exhibits a pronounced maximum around n = 20. In analogy to hydrated magnesium monocations, hydrated aluminum monocations were discussed as Al^I species, $[Al^I(H_2O)_n]^+$. It was postulated that the observed intracluster H_2 formation is associated with an oxidation of Al^I to Al^{III}.[6,7] H_2 elimination was ascribed to the reaction $[Al^I(H_2O)_{20}]^+ \rightarrow [Al^{III}(OH)_2(H_2O)_n]^+ + H_2$. However, Watanabe and Iwata[8] and one of us[9] independently found through ab initio studies of $[Al(H_2O)_{n=1-5}]^+$ that for $n \geq 2$ $[Al^{III}H(OH)(H_2O)_{n-1}]^+$ isomers are significantly more stabilized than those of $Al^+(H_2O)_n$. One would expect the energetically favored isomers to prevail. This seriously questions the prior hypothesis that decay of isolated clusters through H_2 elimination is confined to the "high-energy isomer" $Al^+(H_2O)_n$. Finally, it should be noted in passing that the H_2 elimination from $[Al,11-24H_2O]^+$ was experimentally found to involve concomitant evaporation of two to three H_2O molecules at a time.[7]

Our aim was to find conclusive information whether H_2 elimination from $[Al,20H_2O]^+$ requires oxidation of Al^I or whether it starts from Al^{III}. We performed ab initio studies of the H_2 formation in hydrated Al^{III} and Al^I clusters. We found the reaction to proceed exclusively through hydrated Al^{III} clusters. According to our calculation, H_2 is formed in a multistep intracluster acid−base reaction: $[Al^{III}H(OH)(H_2O)_n]^+ \rightarrow ... \rightarrow [Al^{III}(OH)_2(H_2O)_{n-2}]^+ + H_2$. Our calculations did not reveal any evidence of the H_2 formation being associated with an oxidation of Al^I to Al^{III} within the cluster.

Methods

All calculations were performed in the electronic ground state with density functional theory (DFT). DFT is applicable to fairly large systems, which are out of reach for post-Hartree−Fock-

* To whom correspondence should be adressed. E-mail: bmr@chemie.uni-kl.de, gns@chemie.uni-kl.de.

10.1021/jp020814x CCC: $22.00
Published on Web 07/25/2002

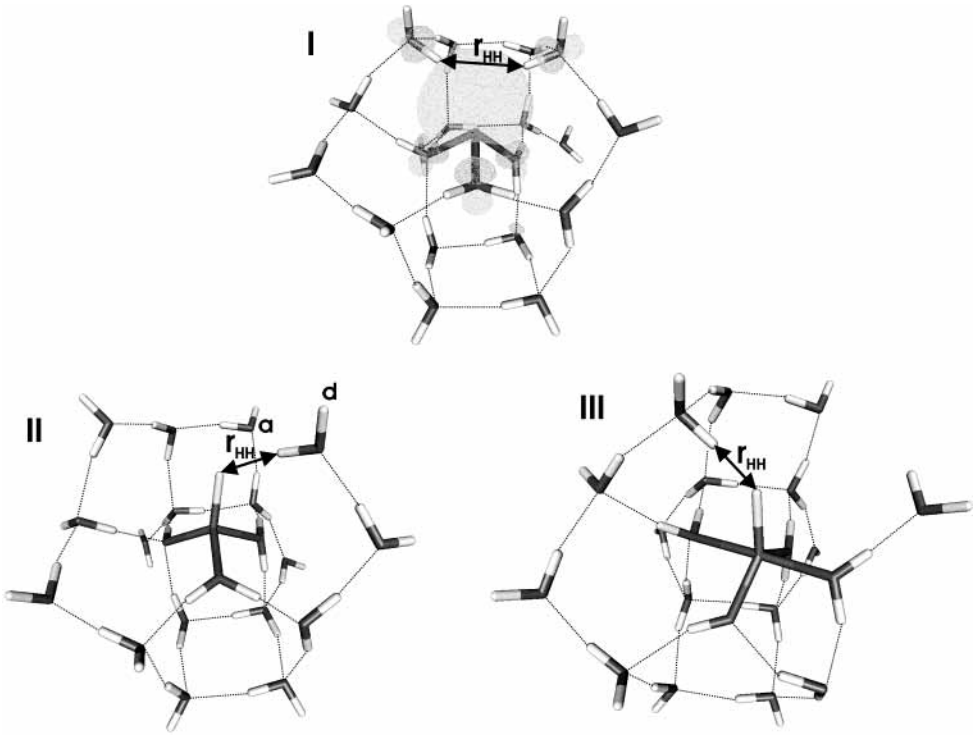

Figure 1. Optimized cluster structures **I**−**III** with stoichiometry $[Al,20H_2O]^+$. In the case of **I**, an isosurface plot of the HOMO is included. Whereas **I** contains an Al^I cation with a formal oxidation state of +1, in **II** and **III** its oxidation state is +3. All clusters contain a H···H motif marked with a double-headed arrow. In **I**, two dangling H atoms of adjacent second-shell H_2O form a tweezer-like structure embracing the HOMO. In structures **II** and **III**, the H···H interaction is between a hydridic H at the Al^{III} cation and a second-shell H_2O molecule. The coordination number of the Al^I cation in **I** is 3 with the HOMO occupying an otherwise "vacant" fourth coordination position. In **II**, the coordination number of the Al^{III} cation is 4; in **III**, it is 5.

based ab initio approaches. In DFT, ionic hydrogen-bonded clusters are generally well-treated because electrostatic interactions clearly dominate over dispersion forces. For our calculations, we chose the Becke88 exchange functional[10] with the Lee, Yang, and Parr gradient-corrected correlation functional[11] (BLYP), which is known to be an efficient density functional with good overall performance. In ab initio molecular dynamics simulation of liquid water, BLYP also proved to yield better agreement with experiment than other gradient-corrected density functionals.[12] For O and H, we employed triple-ζ valence type plus polarization (TZVP) basis sets. For Al, polarization functions of type 2d1f were added (TZVPP). All calculations were performed using the TURBOMOLE[13,14] quantum chemistry program package. The RI "resolution of identity" approximation was applied throughout. The then required auxiliar basis sets were chosen as implemented in TURBOMOLE according to the applied basis sets for O, H, and Al. We performed full geometry optimization of various cluster isomers with the stoichiometry $[Al,20H_2O]^+$. We determined three basic cluster geometries, each of which contains a pair of adjacent H atoms with possible interactions. We parametrically varied this H···H distance (labeled r_{HH} throughout the rest of this paper). To overcome possible basis set limitations in these H···H interactions, the above-described basis sets have been augmented by a floating point (bond function) with a diffuse (3s2p) basis set as developed by Weigend et al.[15]

Results and Discussion

For clusters with the stoichiometry $[Al,20H_2O]^+$, we found three basic cluster structures (Figure 1): **I** $[Al^I(H_2O)_{20}]^+$ (three-fold-coordinated Al^I), **II** $[Al^{III}H(OH)(H_2O)_{19}]^+$ (four-fold-coordinated Al^{III}), **III** $[Al^{III}H(OH)(H_2O)_{19}]^+$ (five-fold-coordinated Al^{III}). Clusters of this size have complex energy hypersurfaces with numerous local minima. Although it is unknown whether any of the determined local minima are global minima, it is certain that the calculated energies for **I**−**III** are characteristic of the respective structure type. We found the total energy to differ only by a few kJ mol^{-1} as long as the total coordination number and the coordinating ligands (H, OH, H_2O) at the aluminum cation were held constant. The composition of the first solvation shell, hereafter labeled as "ionic core", however, has a significant effect on the total energy (Table 1). In **I**, only three H_2O molecules are attached to the aluminum cation in the first solvation shell; the cluster has an $[Al^I(H_2O)_3]^+$ core. The formal oxidation state of the aluminum cation is +1; a lone electron pair remains located at the aluminum monocation (see Figure 1, HOMO in **I**). In contrast to the coexistence of metal dication and a single hydrated electron as found in large $[Mg(H_2O)_n]^+$ clusters, in case of Al_{aq}^+-isomer **I**, a pair of lone electrons remains located at the aluminum cation even in large clusters. The coordination number of the aluminum cation does not exceed 3. This holds true for any cluster isomer of type **I** and for all cluster sizes as large as investigated (25 water molecules). The coordination geometry of the aluminum cation is pyramidal, and the fourth coordination position is occupied

TABLE 1. Relative Enthalpies (T = 0 K) of the Structures I−III[a]

structure	core	ΔH, kJ mol^{-1}
I	$[Al^I(H_2O)_3]^+$	194
II	$[Al^{III}H(OH)(H_2O)_2]^+$	6
III	$[Al^{III}H(OH)(H_2O)_3]^+$	0

[a] Structures **II** and **III** contain the Al^{III} cation. They differ substantially from structure **I** with the Al^I cation. Structure **III** (five-fold-coordinated Al^{III}) is slightly favored with respect to structure **II** (four-fold-coordinated Al^{III})

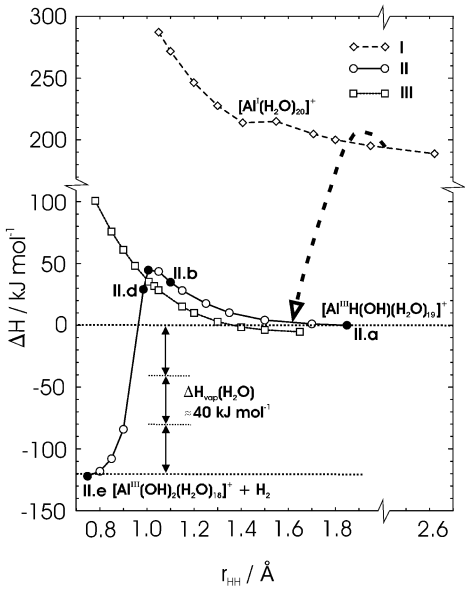

Figure 2. Computed ΔH ($T = 0$ K) for structures **I**−**III** as a function of the H···H coordinate, r_{HH}. In **I** and **III**, shortening of r_{HH} is nonreactive and the H···H interaction becomes repulsive. Only in the case of **II**, H_2 formation is encountered. The activation barrier is 45 kJ mol^{-1} (reaction intermediates **II.a**−**II.c** marked as black circles are shown in Figure 3). The reaction enthalpy $\Delta_r H$ for the elimination of H_2 for **II** is −122 kJ mol^{-1}. This suffices for evaporation of up to three H_2O molecules as observed experimentally.[7] The dashed arrow is meant to indicate that **I** isomerizes into **II** even at large r_{HH}. The activation barrier for this isomerization was calculated to be about 14 kJ mol^{-1} (see text).

by the highest occupied molecular orbital (HOMO), which reveals decent sp-hybrid-like character.

In the case of isomer **II**, the coordination number of the aluminum cation is 4. The coordination geometry is still pyramidal, but one of the H_2O ligands is replaced by OH, and the fourth position is occupied by H. Both OH and H carry significant effective negative charges so that they are referred to as hydroxide, OH^-, and hydride, H^-. Altogether isomer **II** has an $[Al^{III}H(OH)(H_2O)_2]^+$ core.

In isomer **III**, the aluminum cation is coordinated through three H_2O molecules, one hydride, H^-, and one hydroxide, OH^-; the total coodination number is 5. In this case, an $[Al^{III}H(OH)(H_2O)_3]^+$ core is found. Whereas isomers **II** and **III** are similar in total energy, **I** is less stable by a large amount (see Figure 2). In **I**, the formal oxidation state of the aluminum is +1, whereas it is +3 in **II** and **III**. Mulliken population analyses—albeit largely approximate—confirm the differences in the oxidation states (the effective charges (in Coulomb) for Al in the respective structures are the following: **I** (−0.0245), **II** (0.3573), **III** (0.4762)). The obvious lack of energetic stability of isomer **I** makes it very doubtful whether it exists on the time scale of the previously performed experiments (tenth of milliseconds to several seconds within an ion trap).

All cluster structures **I**−**III** contain a structural H···H motif (marked with a two-headed arrow in Figure 1): In **II** and **III**, a second hydration shell located H_2O molecule is pointing with one H atom toward the hydride ion bound to the aluminum cation. In the tweezer structure of **I,** the dangling H atoms of two adjacent H_2O point toward the HOMO located at the aluminum cation. Apparently, there is some attractive interaction between the electrophilic dangling H atoms and the lone electron pair at the Al^I cation. At this point, we like to emphasize the similarities of this structural motif with the HO−H···e$^{\ominus}$···H−OH tweezer structure as found in $[Mg(H_2O)_n]^+$.[3] H_2 formation within the studied clusters requires the approach of any two H atoms, and the question arises which two H atoms react to yield H_2. Because the singular H···H contacts (marked by the double-headed arrow in Figure 1) are signs of attractive interactions, it is fair to assume that H_2 formation—if at all—occurs along the respective H···H coordinate, r_{HH}.

We performed geometry optimizations at fixed H···H distances, r_{HH}, for isomers **I**−**III**. Starting with the relaxed structure, we systematically decreased the H···H distance up to a rise in energy of at most 100 kJ mol^{-1} with respect to the relaxed structure. In Figure 2, the total energies for **I**−**III** are plotted as a function of r_{HH}. In the case of **I** and **III**, there is no indication of any attractive H···H interaction: the computed energies rise steadily. On the basis of our calculations, we rule it unlikely that **I** or **III** are possible structures of $[Al,20H_2O]^+$ to start the experimentally observed dehydrogenation reaction. As indicated by the arrow in Figure 2, we found **I** to isomerize into **II** even at large r_{HH}. If instead of r_{HH} the distance d between the aluminum cation and any of the two H atoms of the marked tweezer structure in **I** was held constant at $d \leq 1.850$ Å, geometry optimizations let structure **I** isomerize into structure **II**. By variation of d, the activation barrier for this transformation was calculated to be about 14 kJ mol^{-1}. At this point, it seems as if structure **I** would be a shallow well in a broad rim that decays on either side into **II**. A more detailed analysis of the transformation of **I** into **II** is in preparation.

In isomer **II**, the forced shortening of r_{HH} induces concomitant structural changes that finally lead to H_2 elimination. The structural changes along the r_{HH} coordinate lead to a minimum energy path as illustrated in Figure 3: Consecutive proton transfers (**II.b**−**II.d**) eventually result in the hydride−oxonium ion adduct **II.d** $[(H_2O)(HO)_2Al-H\cdots H_3O]^+$ at $r_{HH} = 0.985$ Å. If r_{HH} is shortened further, H_2 is formed. At $r_{HH} = 0.900$ Å, H_3O^+ and OH^- have recombined to H_2 and H_2O (**II.e**). The hydrogen molecule is eliminated and a H_2O molecule has taken the vacant coordination position at the aluminum cation. The activation barrier for this reaction is—by inspection of Figure 2—about 45 kJ mol^{-1}.

The proton transfer at $r_{HH} = 1.100$ Å, in which a proton moves into the second solvation shell, creates a first shell OH^- and a second shell H_3O^+ ion. According to our calculations, this is only the very first step in a series of proton transfers, which ultimately result in the formation of H_2. A decrease of r_{HH} below 1.100 Å induces further proton movement through a chain of water molecules to a position adjacent to the nucleophilic hydride ion at the aluminum cation (**II.d**). It is well-known that a proton has a very high "pseudo" mobility through hydrogen-bonded chains of water molecules. This migration is outermost effective through the mere rearrangement of bonds (Grothus mechanism). It is this high mobility of the proton that enables the observed reaction: By the deprotonation of the $[Al^{III}H(OH)(H_2O)_2]^+$ core (which yields the neutral $[Al^{III}H(OH)_2(H_2O)]$ core), a proton is released to the second hydration shell (**II.c**). Net charge migration toward the hydridic H in the then neutral aluminum complex $[Al^{III}H(OH)_2(H_2O)]$ is feasible. This yields an oxonium ion, H_3O^+, adjacent to the hydride ion at the aluminum cation forming the hydride−oxonium ion adduct $[(H_2O)(HO)_2Al-H\cdots H_3O]^+$ (**II.d**). Finally, proton, H^+, and hydride ion, H^-, recombine to form H_2. Thereby, the strongly nucleophilic hydride ion is converted into a hydrogen molecule, which is a considerably weaker nucleophile. Subsequently, H_2 is substituted by a second-shell H_2O molecule (**II.e**). The overall reaction **II.a** → **II.e** comprises an acid (H^+)−base (H^-) reaction. The formal oxidation state of the aluminum cation

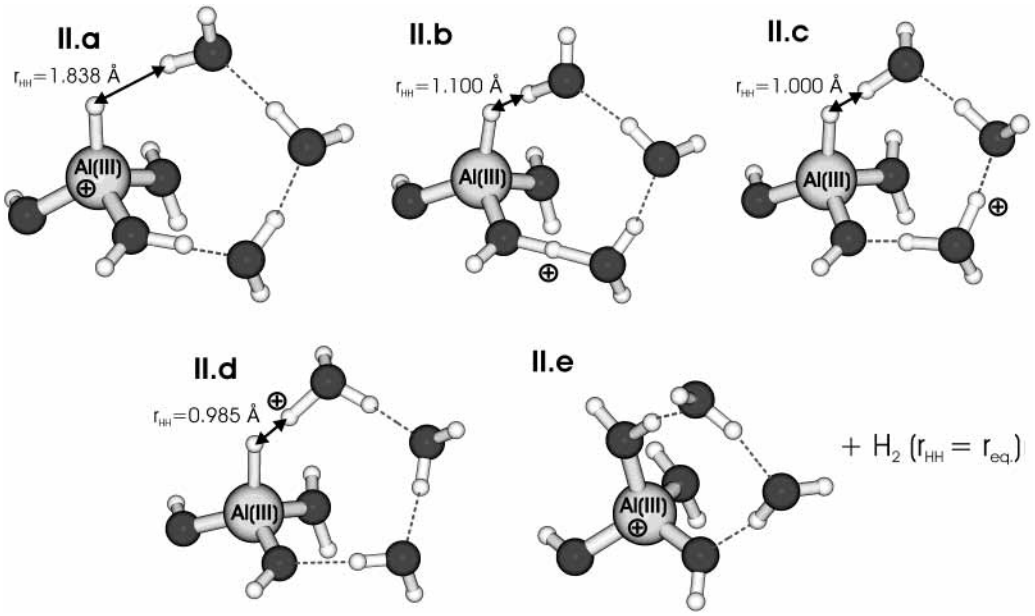

Figure 3. Stucture of the "ionic core" in **II** along the H···H coordinate, r_{HH} (marked by the double-headed arrow). Fourteen more "spectator" water molecules are omitted in this figure but included in all calculations. In the relaxed structure **II.a**, the H···H distance is $r_{HH} = 1.838$ Å. If r_{HH} is shortened to 1.100 Å, a proton is released and a second $Al^{III}-OH$ bond is created in a hydrolysis reaction of a first-shell H_2O molecule: $H_2O \rightarrow OH^- + H^+$ (**II.b** to **II.c**). The proton forms an oxonium ion H_3O^+ within the second solvation shell (**II.c**). If r_{HH} is shortened further, a proton transfer takes place resulting in the hydride−oxonium ion adduct $[(H_2O)(HO)_2Al-H\cdots H_3O]^+$ (**II.d**). Effective proton migration is enabled by the mere rearrangement of hydrogen bonds between adjacent H_2O molecules. The net charge migration is also indicated qualitatively. As soon as r_{HH} is shortened below 0.985 Å, the proton and the hydride ion in $Al^{III}-H^-$ recombine to H_2, which switches with an adjacent H_2O and escapes (**II.e**).

remains unchanged throughout this reaction. It is +3 both in product and in educt clusters. In the bulk phase, the hydrated Al^{III} ion forms the cation acid, $[Al(H_2O)_6]^{3+}$ ($pK_a = 4.76$). In the very first step of the studied cluster reaction, a polarized $Al^{III}-OH_2$ bond is transformed into an $Al^{III}-OH$ bond and the released proton forms an oxonium ion within the second solvation shell. This is a true analogue to a classical hydrolysis reaction, $H_2O \rightarrow OH^- + H^+$, as it can be observed, for example, for the cation acid $[Al(H_2O)_6]^{3+}$ in the bulk phase.[16] In this respect, the $[Al^{III}H(OH)(H_2O)_2]^+$ core also seems to be amphoteric.

In the course of the H_2-elimination reaction, the $Al^{III}-H$ bond is replaced by an $Al^{III}-OH$ bond. The computed energetics for this process are provided in Figure 4. The formation of a second $Al^{III}-OH$ bond (1557 kJ mol^{-1}) and the H_2 formation (1761 kJ mol^{-1}) compensate the energies that are required for the breakage of an $Al^{III}-H^-$ bond (1489 kJ mol^{-1}) and for the hydrolysis of a H_2O molecule (1700 kJ mol^{-1}). De- and rehydration enthalpies are comparable, 978 and 971 kJ mol^{-1}, respectively. The reaction enthalpy (at $T = 0$ K) is computed to be $\Delta_r H = -122$ kJ mol^{-1}. Note that the thermochemical cycle balances exactly. In this process, the swift elimination of the H_2 molecule out of the cluster is a cluster-size-specific feature. Because of additional caging effects, one can expect the hydrogen elimination to be sterically somewhat more demanding in larger clusters. This might lead to an explanation why for even larger cluster sizes ($n > 24$) no decay through H_2 elimination was observed experimentally.

The obtained reaction enthalpy, $\Delta_r H = -122$ kJ mol^{-1}, is in excellent agreement with the experimental observation[7] that H_2 elimination is typically associated with the evaporation of two to three H_2O molecules. When H_2 is formed within the cluster, $\Delta_r H$ is set free. A minor part is released through the kinetic energy of the eliminated H_2. All of the rest leads to vibrational excitation of the cluster. Relaxation of this "heat" is then achieved by evaporative cooling. The evaporation of a single water monomer consumes the negative of the binding energy

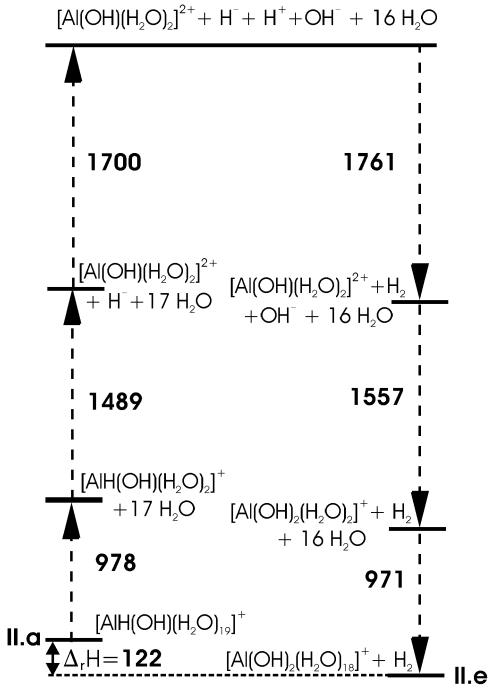

Figure 4. Thermochemical cycle of the H_2 elimination in **II**, ΔH ($T = 0$ K) values in kJ mol^{-1}. The formation of a second $Al^{III}-OH$ bond and the H_2 formation compensate the energy required for the breakage of a $Al^{III}-OH$ bond and for the hydrolysis of a first-shell H_2O molecule.

of a H_2O molecule to the ionic water cluster of that size ($\Delta H_{vap} \approx 40$ kJ mol^{-1}),[17] which is almost identical to the heat of sublimation from bulk ice. If **I** were the reactive cluster species and H_2 would form according to $[Al^{I}(H_2O)_{20}]^+ \rightarrow [Al^{III}(OH)_2(H_2O)_{18}]^+ + H_2$, the reaction enthalpy would be $\Delta_r H = -311$ kJ mol^{-1}. In this case, $\Delta_r H$ would suffice for the evaporation of about seven H_2O molecules, which is neither observed experimentally nor did we find any evidence of H_2 formation from structure **I** through our calculations. In **II**, a proton-transfer

mechanism leads to the hydride−oxonium ion adduct **II.d**, $[(H_2O)(HO)_2Al-H\cdots H_3O]^+$, which decays by formation of H_2. A prerequisite for proton migration in chains of water molecules is the possibility of breaking and forming of hydrogen bonds. This prerequisite is fulfilled for **II**. For example, the formation of the hydride−oxonium ion adduct $[(H_2O)(HO)_2Al-H\cdots H_3O]^+$ through proton transfer (**II.a**−**II.d**) is associated with the hydrogen atom marked as "d" (see Figure 1) slowly aligning with the acceptor molecule "a". Thereby, a new hydrogen bond is established. This may be necessary to stabilize the oxonium ion (see Figure 3, structure **II.d**) by providing a complete first solvation shell. The coordination number of the aluminum cation both in product and in educt cluster is 4; the coordination geometry is tetraedic.

Why is there no evidence of H_2 formation in structure **III** with a five-fold-coordinated Al^{III} cation? The hydride ion—although one of the most basic elemental ions—has a comparatively large ion radius (∼2 Å) and is highly polarizable.[16] In H_2 eliminated $[Al^{III}(OH)_2(H_2O)_{18}]^+$ clusters in which H^- is replaced by a much less polarizable OH^- ion, the Al^{III} cation favors four-fold-coordination. Lower coordination numbers are generally favored for sterical reasons especially when electrostatic repulsion between charged ligands prevails. Isomers with an $[Al^{III}(OH)_2(H_2O)_2]^+$ core are significantly lower in energy (max 46 kJ mol^{-1}) than those with the $[Al^{III}(OH)_2(H_2O)_3]^+$ core with a five-fold-coordinated Al^{III} cation. Assuming a similar reaction mechanism for the H_2 elimination from **III** as from **II**, we would have to postulate intermediates with an $[Al^{III}H(OH)_2(H_2O)_2]$ core (in analogy to **II.c** in Figure 3). Three of the ligands (the hydridic H and the hydroxyl ions) carry negative partial charges, which leads to enhanced Coulomb repulsion. For simple geometric reasons, the Coulomb repulsion in $[Al^{III}H(OH)_2(H_2O)_2]$ would be higher than in tetraedic intermediates of **II**. Therefore, we conclude that the nonreactivity of **III** is largely due to a significantly higher Coulomb repulsion in five-fold-coordinated intermediates.

In previous ICR decay experiments, the cluster with the stoichiometry $[Al,20H_2O]^+$ was most efficient in H_2 formation. Nevertheless, decay by fragmentation was also observed. As one quintessence of our calculations, we find that in $[Al,20H_2O]^+$ energetically similar isomers (e.g., **II** and **III**) may indeed decay through different pathways. The activation barrier of about 45 kJ mol^{-1} for H_2 elimination in case of **II** can be thermally activated, and this process is expected to take place on a subsecond time scale. According to our findings, isomer **III**, however, decays solely by fragmentation. We propose that the observed branching ratio for a cluster $[Al,nH_2O]^+$ does not only depend on the decay propensities of single isomers but also depends on the isomeric composition of the cluster sample under investigation. Unfortunately, the ICR technique does not offer more direct structural information. Collection of further structural information, for example, through appropriate IR spectroscopic experiments in combination with future theoretical studies would help to elucidate further why H_2 elimination from $[Al,nH_2O]^+$ clusters is restricted to the size range $n \approx 11-24$.

Conclusions

We looked for H_2 elimination from different isomers of the stoichiometry $[Al,20H_2O]^+$ by using gradient-corrected DFT (BLYP). We found three different basic structures for $[Al,20H_2O]^+$: **I** $[Al^I(H_2O)_{20}]^+$ with a three-fold-coordinated Al^I; **II** $[Al^{III}H(OH)(H_2O)_{19}]^+$ with a four-fold-coordinated Al^{III}; **III** $[Al^{III}H(OH)(H_2O)_{19}]^+$ with a five-fold-coordinated Al^{III}. Only in the case of **II**, H_2 elimination took place. The reaction was found to be mediated by a multistep intracluster proton-transfer mechanism. In a first step, H^+ is formed via hydrolysis of a first-shell H_2O molecule. In successive reorganization of the hydrogen-bonding network, this proton is transferred to the hydridic H atom bound to the Al^{III} cation. In an acid−base reaction, H_2 is formed by recombination of proton and hydride ion and $[Al^{III}(OH)_2(H_2O)_{18}]^+$ results. The activation barrier was calculated to be 45 kJ mol^{-1}. Our calculations question preceding speculations in which H_2 formation was postulated to be due to an oxidation of the aluminum cation. We found a conclusive mechanism for the formation of H_2 in hydrated Al^{III} clusters but no indication for a reaction in hydrated Al^I clusters.

References and Notes

(1) Akitt, J. W.; Elders, J. M. *J. Chem. Soc., Faraday Trans*. **1985**, *1*, 1923.
(2) Venturini, M.; Berthou, G. *J. Chem. Soc., Dalton Trans*. **1987**, 1145.
(3) Reinhard, B. M.; Niedner-Schatteburg, G. *Phys. Chem. Chem. Phys*. **2002**, *4*, 1471.
(4) Sanekata, M.; Misaizu, F.; Fuke, K.; Iwata, S.; Hashimoto, K. *J. Am. Chem. Soc*. **1995**, *117*, 747.
(5) Berg, C.; Beyer, M.; Achatz, U.; Joos, S.; Niedner-Schatteburg, G.; Bondybey, V. *Chem. Phys*. **1998**, *239*, 379.
(6) Beyer, M.; Berg, C.; Görlitzer, H. W.; Schindler, T.; Achatz, U.; Albert, G.; Niedner-Schatteburg, G.; Bondybey, V. E. *J. Am. Chem. Soc*. **1996**, *118*, 7386−7389.
(7) Beyer, M.; Achatz, U.; Berg, C.; Joos, S.; Niedner-Schatteburg, G.; Bondybey, V. E. *J. Phys. Chem. A* **1999**, *103*, 671.
(8) Watanabe, H.; Iwata, S. *J. Phys. Chem*. **1996**, *100*, 3377.
(9) Niedner-Schatteburg, G. Habilitation Thesis, Technische Universität München, Munich, Germany, 1996.
(10) Becke, A. D. *Phys. Rev. A* **1988**, *38*, 3098.
(11) Lee, C.; Yang, W.; Parr, R. G. *Phys. Rev. B* **1988**, *37*, 785.
(12) Sprik, M.; Hutter, J.; Parinello, M. *J. Chem. Phys*. **1996**, *105*, 1142.
(13) Ahlrichs, R.; Bär, M.; Häser, M.; Horn, H.; Kölmel, C. *Chem. Phys. Lett*. **1989**, *162*, 165.
(14) Arnim, M. V.; Ahlrichs, R. *J. Comput. Chem*. **1998**, *19*, 1746.
(15) Weigend, F.; Ahlrichs, R. *Phys. Chem. Chem. Phys*. **1999**, *1*, 4537.
(16) Holleman, A. F.; Wiberg, E.; Wiberg, N. *Holleman-Wiberg Lehrbuch der Anorganischen Chemie*; Walter de Gruyter: Berlin, 1995.
(17) Shi, Z.; Ford, J. V.; Wei, S.; Castleman, A. W., Jr. *J. Chem. Phys*. **1993**, *99*, 8009.